

Dynamical control of solitons in a parity-time-symmetric coupler by periodic management

Zhiwei Fan^{a,*} and Boris A. Malomed^{a,b}

^a*Department of Physical Electronics, School of Electrical Engineering,
Faculty of Engineering, Tel Aviv University, Tel Aviv 69978, Israel*

^b*Center for Light-Matter Interaction, Tel Aviv University, Tel Aviv 69978, Israel*

We consider a dual-core nonlinear waveguide with the parity-time (\mathcal{PT}) symmetry, realized in the form of equal gain and loss terms carried by the coupled cores. To expand a previously found stability region for solitons in this system, and explore possibilities for the development of dynamical control of the solitons, we introduce “management” in the form of periodic sinusoidal variation of the loss-gain (LG) coefficients, along with synchronous variation of the inter-core coupling (ICC) constant. This system, which can be realized in optics (in the temporal and spatial domains alike), features strong robustness when amplitudes of the variation of the LG and ICC coefficients keep a ratio equal to that of their constant counterparts, allowing one to find exact solutions for \mathcal{PT} -symmetric solitons. A stability region for the solitons is identified in terms of the management amplitude and period, as well as the soliton’s amplitude. In the long-period regime, the solitons evolve adiabatically, making it possible to predict their stability boundaries in an analytical form. The system keeping the Galilean invariance, collisions between moving solitons are considered too. Slowly moving solitons undergo multiple collisions, but eventually separate.

PACS numbers:

Keywords: adiabatic approximation; dual-core waveguides; gain-loss balance; cubic nonlinearity

1. Introduction

One of the most fundamental tenets in physics is the charge-parity-time (\mathcal{CPT}) symmetry, which holds for all Lorentz-invariant systems obeying the causality principle [1, 2]. It implies invariance of the system with respect to the combined parity transformation, \mathcal{P} , which reverses the coordinate axes; charge conjugation, \mathcal{C} , which swaps particles and antiparticles; and time reversal, \mathcal{T} . Its reduced forms, such as \mathcal{PT} and \mathcal{CP} symmetries, may be violated in specific situations, but they also play a profoundly important role in many physical theories. The usual proof of the presence of the latter symmetries is performed to Hermitian Hamiltonians, whose eigenvalues are always real.

However, the invariance of the system with respect to the \mathcal{PT} and \mathcal{CP} transformations does not imply that the underlying Hamiltonian must necessarily be Hermitian. Indeed, it was known from some early examples [3]-[7], and was then discovered, in the systematic form, by Bender and Boettcher [8, 9] (see also review [10] and book [11]) that, in the most general case, Hamiltonians which commute with the \mathcal{PT} operator may include a dissipative (anti-Hermitian) term. Such \mathcal{PT} -symmetric non-Hermitian Hamiltonians often include a complex potential, $U(\mathbf{r})$, whose real and imaginary parts must be, respectively, even and odd functions of spatial coordinates (\mathbf{r}), i.e.,

$$U(-\mathbf{r}) = U^*(\mathbf{r}), \quad (1)$$

where $*$ stands for the complex conjugate. Actually, \mathcal{PT} -symmetric Hamiltonians may admit transformation into Hermitian ones [12, 13]. A well-established fact is that the spectrum of Hamiltonians with complex potentials subject to constraint (1) is real below a critical strength of the imaginary part of the potential, at which the \mathcal{PT} symmetry gets broken, making the system unstable [14] (exceptions in the form of models with *unbreakable* \mathcal{PT} symmetry are known too [15]).

Thus far, the \mathcal{PT} symmetry was not directly realized in quantum systems with complex potentials. On the other hand, a possibility to realize it was predicted for classical optical media with symmetrically inserted gain and loss [16]-[30]. This possibility is based on the commonly known similarity between the quantum-mechanical Schrödinger equation and the propagation equation for optical waveguides, written in the paraxial approximation. Following these ideas, the \mathcal{PT} symmetry was experimentally implemented in various optical and photonic systems [31]-[35]. Emulation of the \mathcal{PT} symmetry was also predicted in atomic Bose-Einstein condensates (BECs), assuming that the gain may be provided by elements working as matter-wave lasers [36].

*Electronic address: zhiweifan1994@gmail.com

As concerns the emulation of fundamental properties of quantum systems in terms of classical optics and in semi-classical BEC, (quasi-) \mathcal{CP} symmetries may be implemented too, in continuous [37–39] and discrete [40] media alike.

The \mathcal{PT} symmetry in an optical waveguide (as well as its \mathcal{CP} counterpart) may naturally combine with the material Kerr nonlinearity, giving rise to propagation models based on cubic nonlinear Schrödinger equations (NLSEs) with the complex potentials subject to condition (1). These models may generate \mathcal{PT} -symmetric solitons, which were addressed in many theoretical works [18], [23]–[59], [15] (see also reviews [41, 42]), and experimentally demonstrated too [34]. Although the presence of the gain and loss makes \mathcal{PT} -symmetric media dissipative, solitons exist in them in continuous families, similar to the commonly known situation in conservative models [43], while usual dissipative solitons exist as isolated solutions (*attractors*, if they are stable) [44].

One of basic settings for the realization of the \mathcal{PT} structure is provided by dual-core waveguides (couplers), with the gain and loss separately placed in parallel cores, which are coupled by tunnelling of the field (light, in optics, or matter waves, in BEC). Stable solitons in conservative couplers with the Kerr nonlinearity were predicted decades ago. These solitons may be symmetric or asymmetric with respect to the identical cores, the symmetry-breaking bifurcation happening at a critical value of the soliton’s total energy/norm (in terms of optics/BEC) [45–48], see also a review in Ref. [49].

A remarkable property of the model of the coupler which includes the cubic nonlinearity in each core, and the above-mentioned \mathcal{PT} -symmetric terms, in the form of the linear gain and loss in the two cores, is that \mathcal{PT} -symmetric and antisymmetric solitons not only can be found in an analytical form, but also their stability region can be identified in an exact form [24, 25] (this region is finite for the symmetric solitons, while antisymmetric ones are completely unstable, although their instability may be weak). Unlike the conservative counterpart of the system, asymmetric solitons cannot exist in the presence of the gain and loss, because asymmetry between components of the soliton in the amplified and damped cores does not admit establishment of the balance between the gain and loss.

Expansion of the stability region for \mathcal{PT} -symmetric solitons and, more generally, developing methods for dynamical control of the solitons is a relevant problem. One potential possibility is suggested by the use of the “management” technique, i.e., periodic modulations of the loss-gain (LG) and inter-core-coupling (ICC) coefficients. In terms of the conservative model of the nonlinear coupler, the management scheme, which corresponds to $\gamma_0 = \gamma_1 = 0$ and $\delta > 0$ in Eq. (2), see below, was introduced in Ref. [50], where effects of the management on symmetric and asymmetric solitons and the transition between them were studied. Similar management schemes are well known to stabilize otherwise unstable or fragile solitons in other settings, such as the *dispersion management* applied to solitons in single-core waveguides (the local dispersion coefficient with a periodically flipping sign [51, 52]), or the stabilization of two-dimensional solitons (which are otherwise unstable against the critical collapse [53]) by means of periodic nonlinearity management [54–56]. In Ref. [57] a particular realization of the above-mentioned management format, implemented as periodic sign change of the LG and ICC coefficients, was applied to the stabilization of symmetric solitons in the \mathcal{PT} -*supersymmetric* coupler with the cubic intra-core nonlinearity and equal LG and ICC coefficients (the supersymmetry implies setting $\gamma_0 = 1$ in terms of Eq. (2) with $\gamma_1 = \delta = 0$, see below). In the supersymmetric coupler with constant parameters, all solitons are unstable (see Eq. (7) below), while the application of the management creates a stability region for them in the corresponding parameter space. Another application of the management to \mathcal{PT} -symmetric solitons was recently elaborated in terms of the single NLSE, with a localized complex potential, satisfying condition (1) and subject to cosinusoidal modulation [58].

The aim of the present work is to explore the stabilization and dynamical control of solitons in the \mathcal{PT} -symmetric nonlinear coupler by means of the management applied in a general form, which combines constant and periodically varying terms in the LG and ICC coefficients. Stability regions for \mathcal{PT} -symmetric solitons are identified by means of systematic simulations, and also in an analytical form, with the help of the adiabatic approximation, in the case of the long-period management format. While the straightforward addition of the management to the system modeling the \mathcal{PT} -symmetric nonlinear coupler leads to shrinkage of the stability area, defined in terms of the soliton’s amplitude (as can be seen below in Figs. 5, 6, and 7(a)), the periodic modulation makes it possible to find stable soliton in new situations – in particular, in those when the average value of the gain and loss is zero ($\gamma_0 = 0$, in terms of Eqs. (2)), as shown below in Figs. 1(a), 4(a), and 5(d), as well as in the case when the ICC coefficient may periodically change its sign, which corresponds to $\delta > 1$, in terms of Eqs. (2) (see Figs. 5(a-c), 6, 7(a), and 8 below). Collisions between moving stable solitons are also considered, by dint of direct simulations.

The rest of the paper is arranged as follows. The model is introduced in Section 2. The main results, both numerical and analytical, which determine stability regions for the \mathcal{PT} -symmetric solitons, are presented in Section 3. Collision between stable solitons are addressed in Section 4. The paper is concluded by Section 5.

2. The model

We consider the propagation of optical or matter waves in the dual-core system described by coupled NLSEs for wave amplitudes $u(z, t)$ and $v(z, t)$ in the cores which carry, severally, gain and loss:

$$\begin{aligned}
i \frac{\partial u}{\partial z} + \frac{1}{2} \frac{\partial^2 u}{\partial t^2} + |u|^2 u - i \left[\gamma_0 + \gamma_1 \sin \left(\frac{2\pi}{L} z \right) \right] u + \left[1 + \delta \sin \left(\frac{2\pi}{L} z + \varphi \right) \right] v &= 0, \\
i \frac{\partial v}{\partial z} + \frac{1}{2} \frac{\partial^2 v}{\partial t^2} + |v|^2 v + i \left[\gamma_0 + \gamma_1 \sin \left(\frac{2\pi}{L} z \right) \right] v + \left[1 + \delta \sin \left(\frac{2\pi}{L} z + \varphi \right) \right] u &= 0.
\end{aligned} \tag{2}$$

In terms of optics, z is the propagation distance, while t is the reduced time in the optical model realized in the temporal domain, as a dual-core optical fiber [48, 49], or the transverse coordinate in a dual-core planar waveguide, which represents the coupler in the spatial domain. The group-velocity-dispersion and Kerr coefficients in Eq. (2) are scaled to be one, assuming that the dispersion has the anomalous sign, which is necessary for maintaining bright solitons; in the spatial domain, the same term represents paraxial diffraction.

The management format, applied to the ICC and LG coefficients, includes constant terms, with the constant part of the former parameter scaled to be 1, and $\gamma_0 < 1$ being the constant part of the latter one. The ICC and LG modulation amplitudes are, respectively, δ and γ_1 , which may be introduced with a phase shift, φ , and L is the modulation period. Because swapping the two cores of the coupler represents the spatial reflection in the present setting, and the propagation distance is the evolution variable in guided-wave-propagation models, Eqs. (2) are invariant with respect to the \mathcal{PT} transformation, $(u, v) \rightarrow (v^*, u^*)$, $z \rightarrow L/2 - z$, the shift of z by $L/2$ being a specific feature added by the management (in other words, $z - L/4$ plays the role of time in the \mathcal{T} transformation).

The dissipative coefficients and δ are defined to be non-negative, without the loss of generality:

$$\gamma_0 \geq 0, \quad \gamma_1 \geq 0, \quad \delta \geq 0 \tag{3}$$

(values $\delta < 0$ and φ are tantamount to $-\delta$ and $\varphi + \pi$). Note, however, that the full local LG and ICC coefficients, i.e., $\gamma_0 + \gamma_1 \sin(2\pi z/L)$ and $1 + \delta \sin(2\pi z/L)$, respectively, may take negative values – in particular, because we will consider, among others, the cases of $\gamma_0 = 0$ and $\delta > 1$.

In the absence of the management, $\gamma_1 = \delta = 0$, a family of exact soliton solutions to Eq. (2) can be easily found [24, 25], provided that $\gamma_0 \leq 1$:

$$v(z, t) = \left(i\gamma_0 \pm \sqrt{1 - \gamma_0^2} \right) u(z, t), \tag{4}$$

$$v(z, t) = A \exp \left[i \left(A^2/2 \pm \sqrt{1 - \gamma_0^2} \right) z \right] \operatorname{sech}(At), \tag{5}$$

where A is an arbitrary amplitude, and signs $+$ and $-$ correspond to the \mathcal{PT} -symmetric and antisymmetric solitons, respectively, which are so named [24] because they correspond, respectively, to the usual symmetric and antisymmetric solitons in the usual coupler's model in the absence of the gain and loss ($\gamma_0 = 0$; note that more general compound solitons, with an arbitrary phase difference between the two components, are not possible, because the \mathcal{P} transformation has only two eigenvalues, $+1$ and -1). Note that solution (4) implies

$$|u(z, t)|^2 = |v(z, t)|^2, \tag{6}$$

which maintains equilibrium between the gain and loss.

The stability region for the exact symmetric solitons in the static model ($\gamma_1 = \delta = 0$), given by Eqs. (4) and (5), can also be found in an exact form [24, 25]: they are stable if the squared amplitude takes values

$$A^2 \leq A_{\text{crit}}^2(\gamma_0) = (4/3) \sqrt{1 - \gamma_0^2}, \tag{7}$$

while the antisymmetric solitons are completely unstable (although their instability may be very weak, depending on the parameters). For this reason, antisymmetric solitons are not considered in detail below (they may be made stable in a discrete version of Eqs. (2) [59]).

As mentioned above, an essential difference of the \mathcal{PT} -symmetric system (2) from its conservative counterpart, with $\gamma_0 = 0$, is that, at $A^2 > A_{\text{crit}}^2$, unstable \mathcal{PT} -symmetric solitons are not replaced by stable asymmetric ones (cf. works [45]-[49], where asymmetric solitons are considered in the conservative system), because asymmetric states, that do not obey condition (6), cannot maintain the LG balance (i.e., asymmetric solitons cannot exist in the case of $\gamma_0 > 0$). As a result, unstable \mathcal{PT} -symmetric soliton suffer blowup, similar to what is shown below in Fig. 2(c).

3. Stabilization and dynamical control of solitons by the management

3.1. Numerical results

We focus on the case of zero phase shift between the variations of the LG and ICC coefficients, i.e., $\varphi = 0$ in Eq. (2), as the management format with $\varphi \neq 0$ (in particular, $\varphi = \pi$, which, as mentioned above, is tantamount to taking $\delta < 0$) leads to strong instability. The stability of the solitons under the action of the management was identified from sufficiently long direct simulations, with the input taken in the form of Eqs. (4) and (5) at $z = 0$ and a given value of γ_0 , while A was varied, to collect systematic results for the stability of the solitons with different amplitudes, cf. Eq. (7). The simulations were carried out by means of the split-step numerical algorithm, similar to those employed in Refs. [24] and [25]. A rigorous study of the stability against small perturbations, which makes it necessary to solve linearized equations around the periodically varying solution, is a challenging task, which we do not tackle here.

A combination of panels displayed in Fig. 1 show stability areas for the solitons with different values of the constant part of the LG coefficient, γ_0 , for a fixed management period, $L = \pi/3$, and two different values of amplitude A in the input expression (5). Naturally, the stability areas are larger for smaller A (similar to what is predicted by Eq. (7) in the absence of the management), and they shrink with the increase of the modulation amplitudes, γ_1 and δ . It is clearly seen that the strongest stability is provided by the management scheme in which the ratio of δ and γ_1 is the same as the ratio of their counterparts in the constant parts of the ICC and LG coefficients (in other words, the management is applied *coherently* with the static part of the system):

$$\delta/\gamma_1 = 1/\gamma_0. \quad (8)$$

This finding is explained by the fact that, when relation (8) holds, Eqs. (2) admit *exact solutions* for \mathcal{PT} -symmetric and antisymmetric solitons:

$$v(z, t) = A \exp \left[i \left(A^2/2 \pm \sqrt{1 - \gamma_0^2} \right) z \mp i \frac{L\gamma_1 \sqrt{1 - \gamma_0^2}}{2\pi\gamma_0} \cos \left(\frac{2\pi}{L} z \right) \right] \operatorname{sech}(At), \quad (9)$$

cf. Eq. (5), with $u(z, t)$ given by exactly the same equation (4) as above. Of course, stability conditions for these exact solutions cannot be found in the same simple form (7) which is valid in the absence of the management.

A principally different case is one shown in Fig. 1(a), which corresponds to $\gamma_0 = 0$ (i.e., the static system is the conservative one). In this case, relation (8) does not exist, and, accordingly, the shape of the stability area is completely different from those displayed in panels (b)-(f).

The evolution of a stable soliton which satisfies constraint (8) is displayed in Fig. 2(a), showing that it keeps a constant shape, in exact agreement with Eqs. (9) and (4). On the other hand, in the case when the management parameters deviate from condition (8), a typical example of the evolution of stable solitons shows small but visible fluctuations in Fig. 2(b). On the contrary, unstable solitons blow up due to the failure of the LG balance, see an example of the quick onset of the blowup in Fig. 2(c), for parameters chosen deep in the instability area. Moderately unstable solitons develop into breathers, which evolve as quasi-stable states (cf. similar dynamical modes reported in Ref. [25]), but eventually they are destroyed by the collapse, as shown in Fig. 3.

Similar results, pertaining to a larger management period, $L = \pi$, are presented in Fig. 4. It is seen that they are qualitatively similar to those in Fig. 1, but the large period supports smaller stability areas, both in the case of $\gamma_0 = 0$ and $\gamma_0 > 0$. Note that the same condition (8) determines the condition of the optimum stability in this case too, when exact \mathcal{PT} -symmetric solitons are given by Eqs. (4) and (9).

Another essential summary of the results is presented in Fig. 5, in the form of stability maps in the plane of (γ_1, A) , while δ is linked to γ_1 by the optimum-stability condition (8). At $\gamma_1 = 0$ (hence $\delta = 0$ too), i.e., in the absence the management, the largest values of A admitting the stability in Figs. 5(a) and (b) are precisely the same as predicted analytically by Eq. (7) for the static \mathcal{PT} -symmetric coupler.

A natural trend evidenced by Figs. 5(a) and (b) is that the stability limit, given by the largest value of A up to which the solitons persist, decreases with the increase of the modulation strength, γ_1 . A noteworthy feature observed by Fig. 5(b) is that, for a relatively large management period, $L = \pi$, the stability boundary for larger γ_0 may be located higher, in terms of A , than its counterpart for smaller γ_0 , see, for instance, the boundaries for $\gamma_0 = 0.15$ and $\gamma_0 = 0.5$. This feature is counter-intuitive, as the exact result (7) for the solitons in the static model demonstrates monotonic decay of A_{crit} with the increase of γ_0 . An explanation for this point is that, at smaller γ_0 , the stability is more sensitive to changes of period L . The analysis of the situation for the long-period modulations with large L is presented in the next section, with the help of the adiabatic approximation.

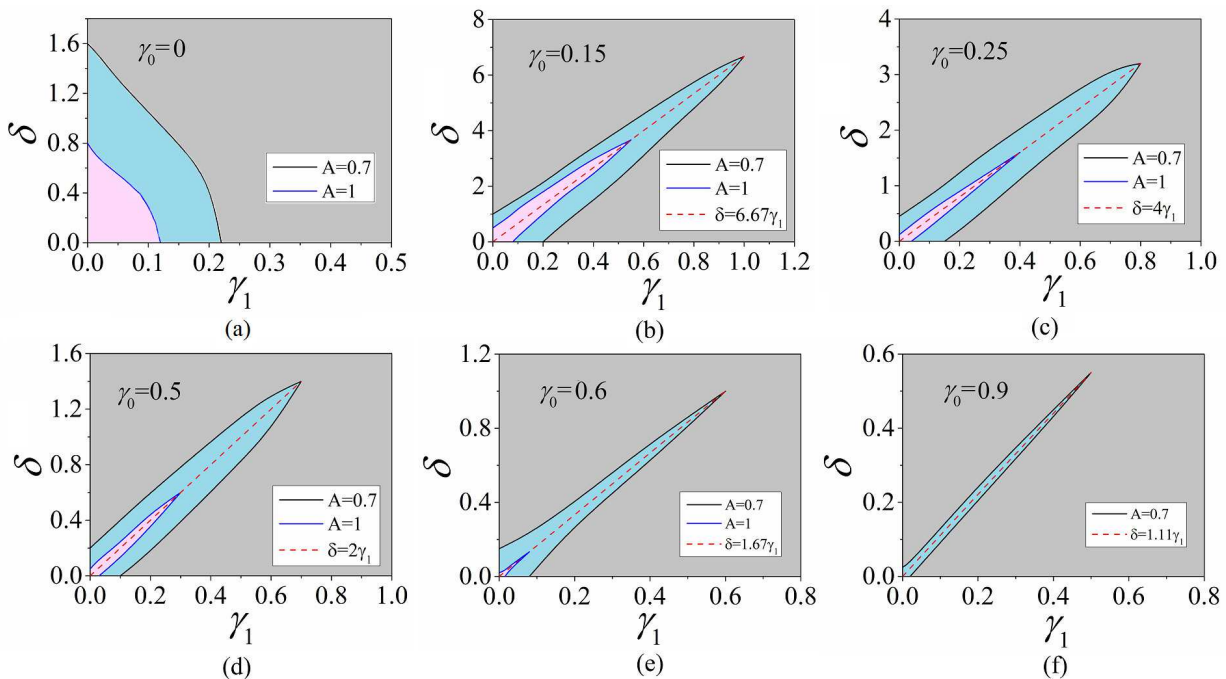


FIG. 1: (Color online) Stability charts for \mathcal{PT} -symmetric solitons under the action of the management with a fixed value of the period, $L = \pi/3$. In panels (a) to (f), the constant part of the LG coefficient is $\gamma_0 = 0, 0.15, 0.25, 0.5, 0.6, 0.9$, respectively. The solitons, with initial amplitudes $A = 0.7$ and 1 in Eq. (5), are stable, respectively, in the blue and pink areas in the plane of the modulation amplitudes, (γ_1, δ) (in the pink areas, both $A = 0.7$ and 1 produce stable solitons). The straight dashed line denotes the optimum-stability relation (8), see the text. The simulations produce unstable evolution in the ambient gray region. In panel (f), there is no stability area for $A = 1$, in agreement with Eq. (7), which yields, in this case, $A_{\text{crit}}^2(0.9) \approx 0.58$.

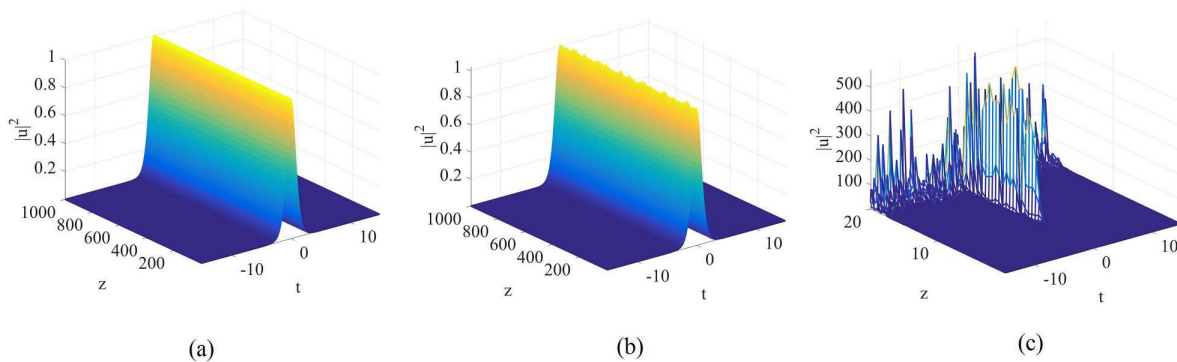


FIG. 2: (Color online) Typical examples of the evolution of stable and unstable solitons under the action of the management, for fixed parameters $(L, \gamma_0, \gamma_1, A) = (\pi/3, 0.5, 0.3, 1)$, while δ is varied. In panel (a), with $\delta = 0.6$, which satisfies the optimum-stability relation (8), the soliton's shape remains unchanged in the course of the propagation, in agreement with Eq. (9). In panel (b), $\delta = 0.64$, which does not meet condition (8) (this δ corresponds to $\gamma_0(\delta/\gamma_1) \approx 1.07$, instead of 1), but belongs to an edge of the stability area in Fig. 1(d). In this case, shape oscillations are small but visible. Panel (c) is an example of the evolution of an unstable soliton with $\delta = 0.1$, which lies deep in the gray area in Fig. 1(d). This soliton blows up due to the imbalance between the gain and loss (note the difference in the vertical scales between panels (a,b) and (c)).

Lastly, Fig. 5(d) demonstrates that, in the case of $\gamma_0 = 0$, when the constant term is absent in the LG coefficient (hence Eq. (8) is irrelevant), the increase of the modulation amplitudes of both the LG and ICC terms, i.e., γ_1 and δ , naturally causes shrinkage of the stability area.

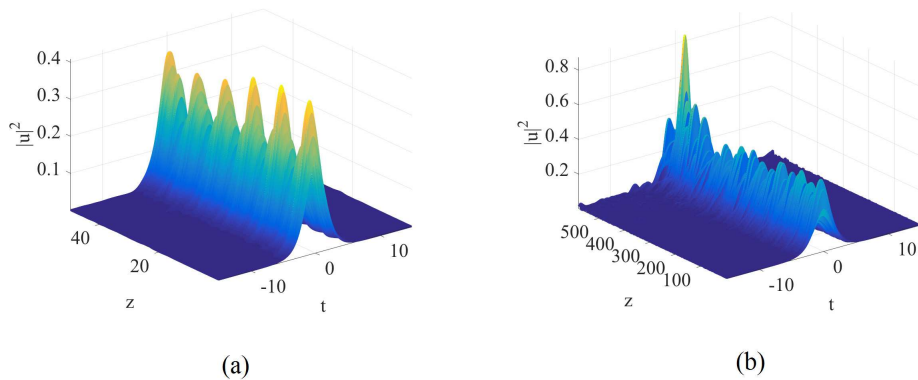


FIG. 3: (Color online) A typical example of the evolution of a moderately unstable breather, for parameters $(L, \gamma_0, \gamma_1, \delta, A) = (\pi, 0.9, 0.2, 0.12, 0.5)$. The breather remains quasi-stable over a short propagation distance in panel (a), but eventually becomes unstable in the course of the further evolution, as shown in panel (b).

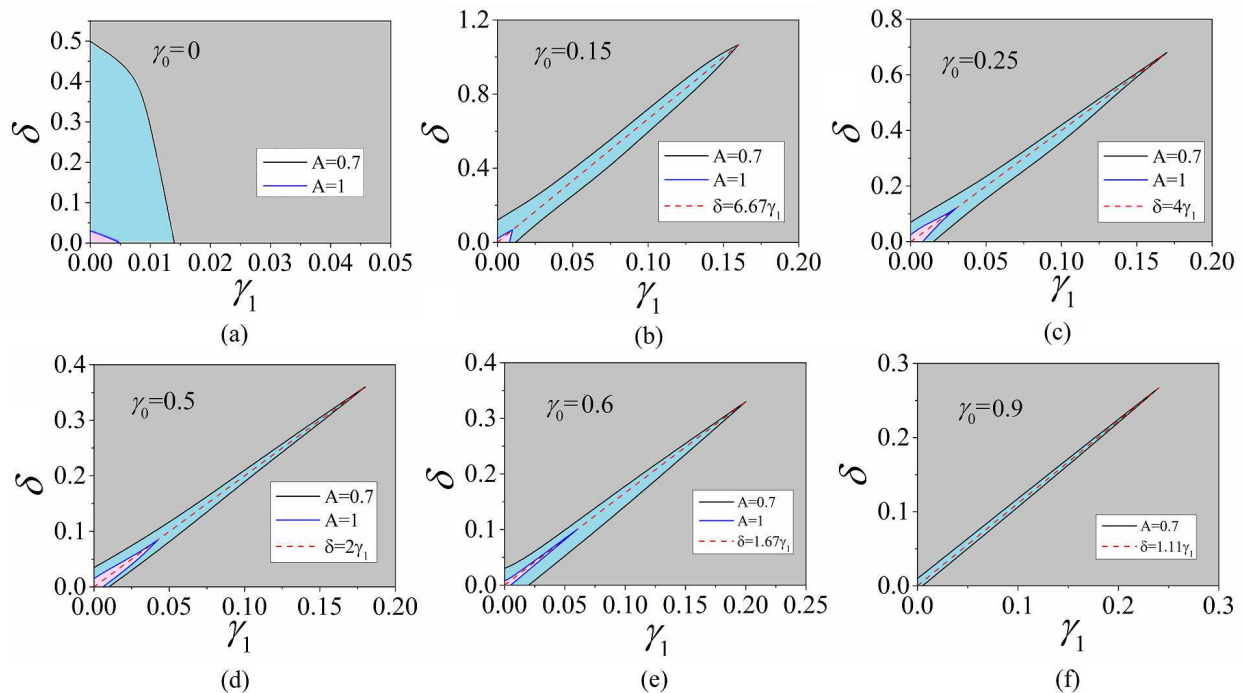


FIG. 4: (Color online) The same as in Fig. 1, but for the management period which is three times as large, $L = \pi$. The structure of the stability domains remains similar, but their overall size essentially decreases, in comparison with the case of $L = \pi/3$. In particular, there is no stability area for $A = 1$ in panel (f), for the same reason as in Fig. 1(f).

3.2. The adiabatic approximation

The long-period management may be considered as adiabatic under the condition that the period is much larger than the intrinsic period of phase oscillations of soliton (5):

$$L \gg 4\pi/A^2. \quad (10)$$

This condition makes it possible to separate the scales of the slow evolution of stable solitons, driven by the management, and their rapid phase oscillations, which correspond to the nearly-constant values of the parameters

The adiabatic limit allows one to approximately transform Eq. (2) into equations with constant coefficients, by

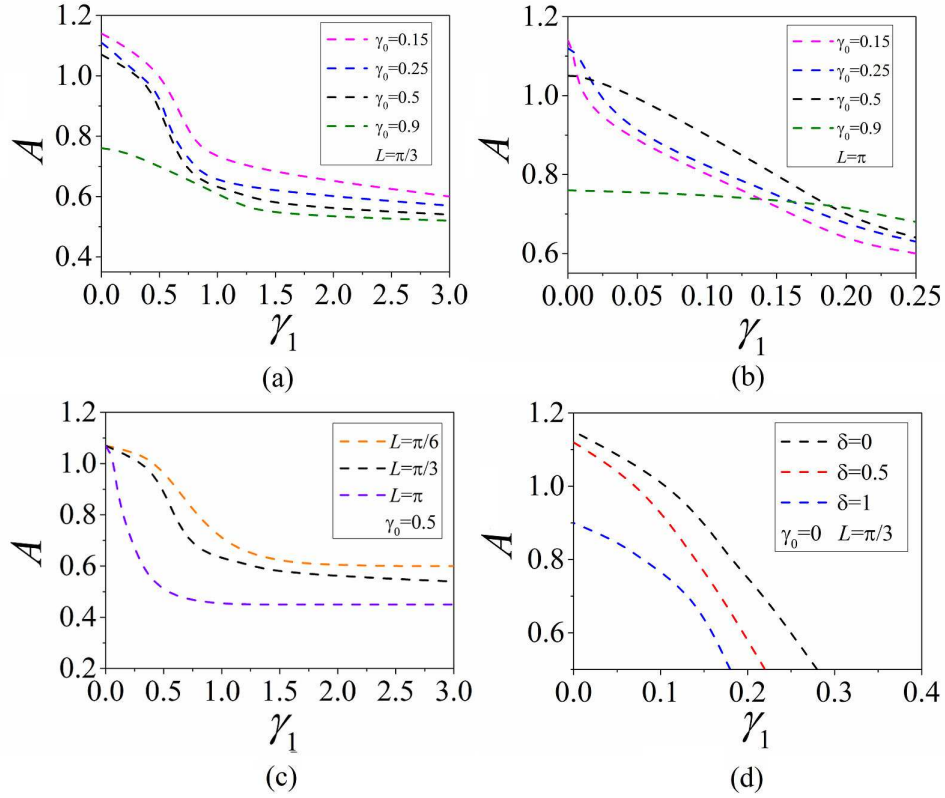


FIG. 5: (Color online) Panels (a,b,c): imposing the optimum-stability condition (8), i.e., $\delta = \gamma_1/\gamma_0$, stability boundaries for \mathcal{PT} -symmetric solitons are displayed in the plane of (γ_1, A) (recall A is the input's amplitude, according to Eq. (5)). The solitons are stable beneath boundaries shown in the panels. Widely different ranges of parameter γ_1 , displayed in panels (a), (c) and (b), (d), correspond to the fact that characteristic values of this parameter are indeed strongly different in the respective cases. In (a) and (b), the management period is fixed, respectively, at $L = \pi/3$ and $L = \pi$, and the results are presented for a set of different values of γ_0 , cf. Figs. 1 and 4. In panel (c), $\gamma_0 = 0.5$ is fixed, and a set of the stability boundaries are displayed for different periods L . Panel (d) is plotted for $\gamma_0 = 0$, for which condition (8) is irrelevant. In this case, the stability boundaries are presented for fixed $L = \pi/3$ and three different values of the amplitude of the ICC modulation: $\delta = 0, 0.5$, and 1.

defining

$$t \equiv \frac{\tilde{t}}{\sqrt{1 + \delta \sin\left(\frac{2\pi}{L}z\right)}}, \quad (11)$$

$$z \equiv \frac{\tilde{z}}{1 + \delta \sin\left(\frac{2\pi}{L}z\right)}, \quad (12)$$

$$(u, v) \equiv (\tilde{u}, \tilde{v}) \sqrt{1 + \delta \sin\left(\frac{2\pi}{L}z\right)}, \quad (13)$$

where it is assumed that γ_1 and δ are related by Eq. (8), to address the case which is most relevant for the stability analysis. The substitution of variables (11)-(13) leads, in the first approximation, to the following equations replacing Eq. (2):

$$i \frac{\partial \tilde{u}}{\partial \tilde{z}} + \frac{1}{2} \frac{\partial^2 \tilde{u}}{\partial \tilde{t}^2} + |\tilde{u}|^2 \tilde{u} - i\gamma_0 \tilde{u} + \tilde{v} = 0, \quad (14)$$

$$i \frac{\partial \tilde{v}}{\partial \tilde{z}} + \frac{1}{2} \frac{\partial^2 \tilde{v}}{\partial \tilde{t}^2} + |\tilde{v}|^2 \tilde{v} + i\gamma_0 \tilde{v} + \tilde{u} = 0.$$

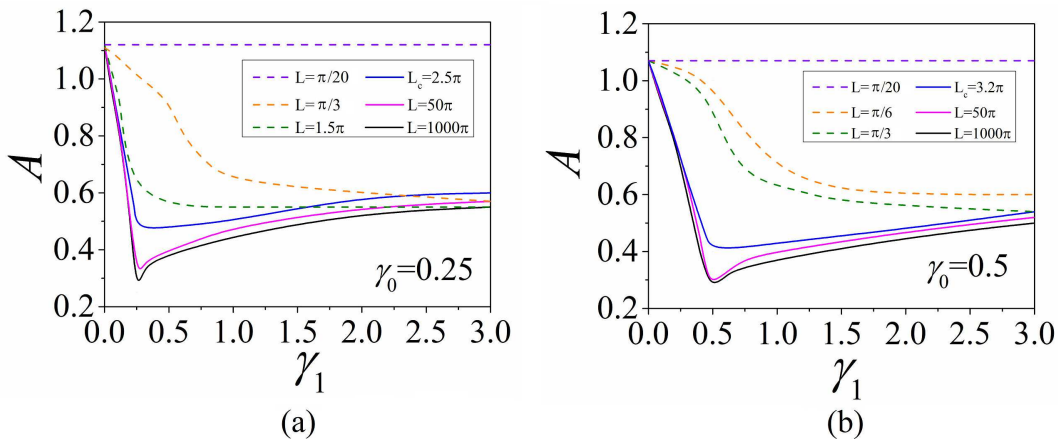


FIG. 6: (Color online) Stability boundaries in the plane of (γ_1, A) under condition (8), for six very different values of the management period, from $L = \pi/20$ to $L = 1000\pi$, and two different values of γ_0 . The stability area shrinks but does not vanish with the increase of L . The shape of the stability boundary becomes non-monotonous (the minimum point appears on it) at $L \geq L_c$. The solid and dashed lines designate the non-monotonous and monotonous stability boundaries, respectively.

This approximate transformation is relevant under condition

$$\delta < 1, \quad (15)$$

which is necessary to secure condition $1 + \delta \sin(2\pi z/L) > 0$; otherwise, the transformation given by (11)-(13) becomes singular. Taking into regard the currently imposed relation (8), Eq. (15) may also be written as $\gamma_1 < \gamma_0$.

Being tantamount in their form to Eq. (2), equations (14) produce solutions in the form of (4) and (5), which, in turn, are stable under the accordingly transformed criterion (7). The critical condition corresponds to the largest amplitude, in terms of the transformed fields (13), which is $\tilde{A}_{\text{crit}}^2 = A^2/(1 - \delta)$, attained at $\sin(2\pi z/L) = -1$. In terms of the original notation, the respective approximate stability criterion for the slowly varying solitons takes the form of

$$A_0^2 < (A_0^2)_{\text{crit}} = \frac{4}{3} \sqrt{1 - \gamma_0^2} (1 - \delta) \equiv \frac{4}{3} \sqrt{1 - \gamma_0^2} \left(1 - \frac{\gamma_1}{\gamma_0}\right) \quad (16)$$

(Eq. (8) is used to write the result in Eq. (16) in two equivalent forms).

The global picture of the transformation of the stability boundary in the plane of (γ_1, A) is illustrated in Fig. (6), by showing it for six different management periods, which cover the range of four order of magnitude (from $L = \pi/20$ to $L = 1000\pi$), and two values $\gamma_0 = 0.25, 0.5$. It is observed that, in each case, there is a critical value, L_c , such that dependence $A(\gamma_1)$ along the stability boundary is monotonous at $L < L_c$, and non-monotonous at $L > L_c$.

Further, the analytical prediction given by Eq. (16) is compared to the numerically found stability boundaries, for a very large period, $L \equiv 1000\pi$, in Fig. 7(a). It is seen that the prediction is close to the numerical counterparts in the region of $\gamma_1 < \gamma_0$. At $\gamma_1 = \gamma_0$ the analytically predicted critical amplitude vanishes in Eq. (16), and it ceases to exist at $\gamma_1 > \gamma_0$, i.e., in the case when the sign of the total LG periodically changes, according to Eq. (2). In fact, the analytical approximation breaks down close to $\gamma_1 = \gamma_0$ (i.e., close to $\delta = 1$, see Eq. (15)), as mentioned above. In fact, the numerically found critical amplitude does not vanish at point $\gamma_1 = \gamma_0$, but, instead, it attains a finite minimum value. At $\gamma_1 > \gamma_0$, the stability area still exists, slowly expanding with the increase of $\gamma_1/\gamma_0 \equiv \delta$. This trend is a natural one, as the increase of the absolute value of the ICC suppresses the symmetry-breaking instability driven by the self-focusing nonlinearity [45]-[49].

At all values of γ_0 , the minimum of A_{crit} is attained exactly at $\gamma_1 = \gamma_0$, in full agreement with the analytical prediction. This fact is confirmed by the numerically generated value of γ_0/γ_1 at the minimum point, which is shown, versus L , by the dashed line in Fig. 7(b). As concerns value A_{min} of the critical amplitude at the minimum point, it slowly decreasing with the increase of L , as is also shown in Fig. 7(b).

4. Collisions of solitons

Because Eq. (2) keeps the Galilean invariance, a stable soliton can be set in motion by applying kick η to it, i.e., multiplying the quiescent solution $\{u_0(z, t), v_0(z, t)\}$ by $\exp(i\eta t)$. As a result, it will be transformed into a moving

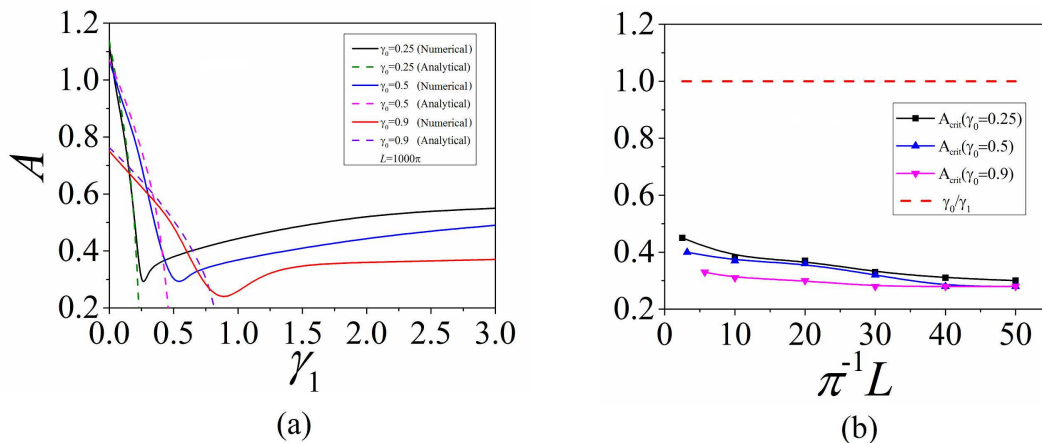


FIG. 7: (Color online) (a) Stability boundaries in the plane of (γ_1, A) under condition (8), at a very large fixed management period, $L = 1000\pi$, and three different values of γ_0 . Solid and dashed lines represent, severally, numerical results and analytical ones predicted by Eq. (16). (b) Value A_{crit} of the amplitude at the minimum point vs. L , at three different values of γ_0 . The horizontal dashed line shows the value of γ_0/γ_1 at the minimum point, confirming that it exactly corresponds to $\gamma_1 = \gamma_0$, as predicted by the analytical approximation.

one,

$$\{u_\eta, v_\eta\} = \{u_0(z, t - cz), v_0(z, t - cz)\} \exp(-i/2 c^2 z), \quad c = \eta. \quad (17)$$

This fact suggests to simulate collisions between initially separated solitons, boosted in opposite directions by kicks $\pm\eta$, cf. Refs. [24] and [25].

A typical set of collisions, simulated for a set of different values of the kicks, is displayed in Fig.(8). Panels(a) to (f) show different outcomes of the collisions, produced by increasing values of η . In all the cases, the colliding solitons eventually separate. However, in panels (a) and (b) slowly moving soliton pairs form quasi-bound states, in which they perform several oscillations before re-emerging with larger values of opposite velocities $\pm c$ (see Eq. (17)) than they had prior to the collision. The formation of the intermediate bound state resembles the effect which was previously found in simulations of soliton-soliton collisions in other nonintegrable models [60–62]. Fast moving solitons, boosted by stronger kicks, pass through each other elastically (panels (d,e,f)), which is typical for collisions between solitons in conservative systems [62], and remains true in the present \mathcal{PT} -symmetric one.

Lastly, Fig. 9 displays simulations of the collisions with the same values of L , γ_0 , and A , under the action of the same kicks as in the top row in Fig. 8, but in the absence of the management, i.e., for $\gamma_1 = \delta = 0$. It is clearly seen that the collisions are completely elastic (similar to those simulated in [24]), and the intermediate quasi-bound states do not emerge. Thus, the presence of the management accounts for the creation of the those states. For larger kicks, corresponding to the bottom row in Fig. 8, the collisions remain the same (elastic) as displayed in Fig. 8.

As said above, in this work we do not address \mathcal{PT} -antisymmetric solitons, which correspond to the bottom signs in Eqs. (4), (5) and (9), as they are unstable even in the absence of the management. The instability of some antisymmetric solitons being weak, it is possible to consider their collisions too, with each other or with \mathcal{PT} -symmetric counterparts. As shown in Ref. [25], in the latter case the collision may excite intrinsic oscillations in the solitons. The consideration of this case is beyond the scope of the present work.

5. Conclusion

The objective of this work is to generalize the known model of the \mathcal{PT} -symmetric coupler, based on linearly coupled waveguides with the intrinsic cubic nonlinearity and equal gain and loss coefficients carried by the guiding cores. The generalization introduces “management”, which makes the LG (loss-gain) and ICC (inter-core-coupling) coefficients periodically varying functions of the evolutionary variable. The model may be realized in optics, in the temporal and spatial domains alike. Stability of \mathcal{PT} -symmetric solitons and possibilities of applying the dynamical control to them by means of the management are explored by means of systematic simulations, and also analytically in the adiabatic approximation, which corresponds to the long-period limit. The stability is strongest when the ratio of the amplitudes of the modulation of the LG and ICC coefficients is equal to its counterpart for the constant parts of the same coefficients. In the latter case, an exact solution is found for \mathcal{PT} -symmetric solitons. Collisions between moving solitons were briefly considered too.

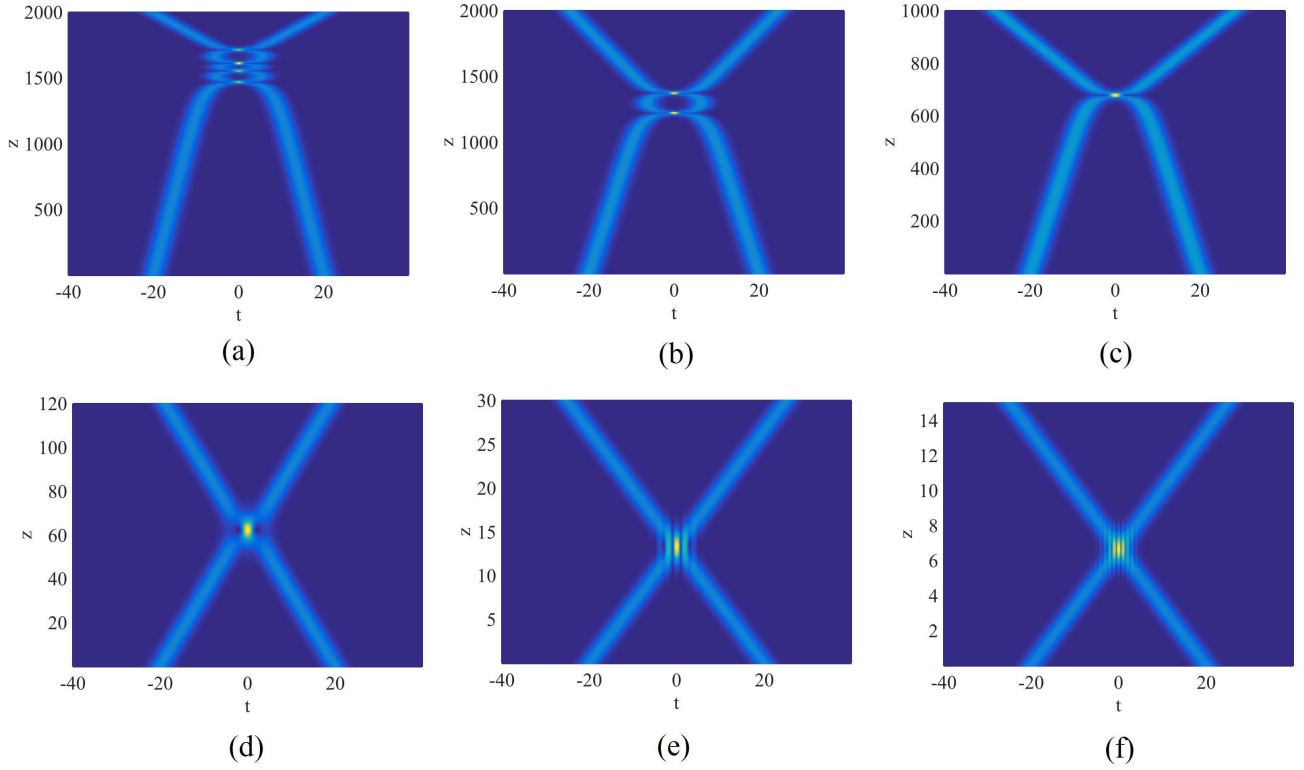


FIG. 8: (Color online) Typical examples of collisions between identical stable \mathcal{PT} -symmetric solitons moving in opposite directions under the action of kicks $\pm\eta$, see Eq. (17). The solitons' parameters are $(L, \gamma_0, \gamma_1, \delta, A) = (\pi/3, 0.5, 1, 2.05, 0.5)$. From panel (a) to (f), the kicks applied to the soliton pairs are $\eta = \pm 0.008, \pm 0.01, \pm 0.02, \pm 0.3, \pm 1.5, \pm 3$, respectively.

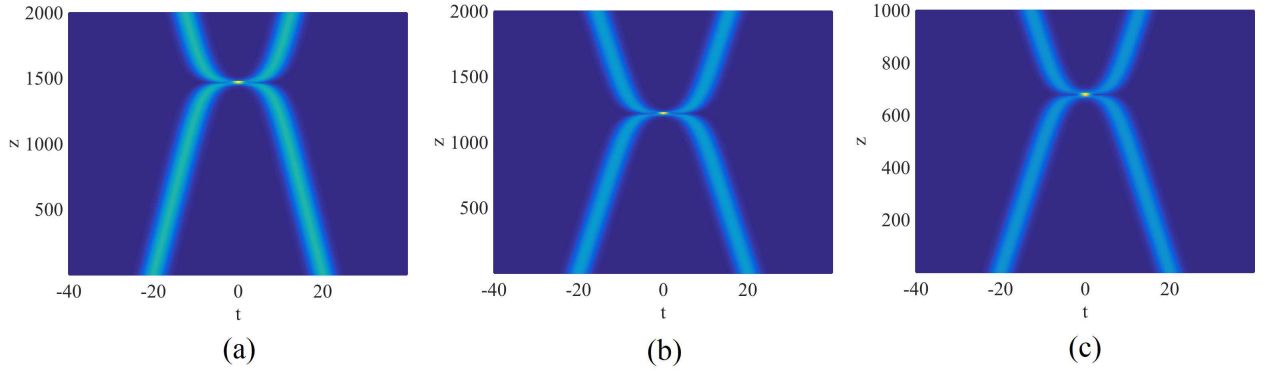


FIG. 9: (Color online) The same as in the top row of Fig. 8, but in the absence of the management, i.e., with $\gamma_1 = \delta = 0$, while other parameters, including the kicks, keep the same values.

A challenging possibility for the development of the present analysis is to develop analysis of the management for solitons in two-dimensional \mathcal{PT} -symmetric systems.

Acknowledgments

This work was supported, in part, by the Israel Science Foundation through grant No. 1287/17. We appreciate a helpful discussion with Zhaopin Chen (Tel Aviv University) and technical assistance provided by Ms. Shiyue Liu

(Chinese University of Hong Kong).

- [1] Bernabeu J. \mathcal{T} and CPT symmetries in entangled neutral meson systems. J Phys: Conf Ser 2011;335:012011.
- [2] Yaffe LG. Particles and Symmetries. Seattle: University of Washington Press; 2013.
- [3] Feshbach H, Porter C, Weisskopf V. Model for nuclear reactions with neutrons. Phys Rev 1954;96:448.
- [4] Sudarshan ECG, Chiu CB, Gorini V. Decaying states as complex energy eigenvectors in generalized quantum mechanics. Phys Rev D 1978;18:2914-2929.
- [5] Moiseyev N, Certain P, Weinhold F. Resonance properties of complex-rotated Hamiltonians. Mol Phys 1978;36(6):1613-1630.
- [6] Scholtz F, Geyer H, Hahne F. Quasi-Hermitian operators in quantum mechanics and the variational principle. Ann Phys 1992;213:74-101.
- [7] Dorey P, Dunning C, Tateo R. Spectral equivalences, Bethe ansatz equations, and reality properties in \mathcal{PT} -symmetric quantum mechanics. J Phys A: Math Gen 2001;34:5679-5704.
- [8] Bender CM, Boettcher S. Real spectra in non-Hermitian Hamiltonians having \mathcal{PT} symmetry. Phys Rev Lett 1998;80:5243-5246.
- [9] Bender CM, Brody DC, Jones HF. Complex extension of quantum mechanics. Phys Rev Lett 2002;89:270401.
- [10] Bender CM. Making sense of non-Hermitian Hamiltonians. Rep Prog Phys 2007;70:947-1018.
- [11] Moiseyev N. Non-Hermitian Quantum Mechanics. Cambridge University Press; 2011.
- [12] Mostafazadeh A. Metric operators for quasi-Hermitian Hamiltonians and symmetries of equivalent Hermitian Hamiltonians. J Phys A: Math Gen 2008;41:244017.
- [13] Barashenkov IV. Hamiltonian formulation of the standard \mathcal{PT} -symmetric nonlinear Schrödinger dimer. Phys Rev A 2014;90:045802.
- [14] Yang J. Symmetry breaking of solitons in one-dimensional parity-time-symmetric optical potentials. Opt Lett 2014;39:5547-5550.
- [15] Lutsky V, Luz E, Granot E, Malomed BA. Making the \mathcal{PT} symmetry unbreakable. In: Christodoulides D, Yang J. Parity-time Symmetry and Its Applications, Singapore: Springer; 2018, p. 443-464.
- [16] Ruschhaupt A, Delgado F, Muga JG. Physical realization of \mathcal{PT} -symmetric potential scattering in a planar slab waveguide. J Phys A: Math Gen 2005;38:171-176.
- [17] El-Ganainy R, Makris KG, Christodoulides DN, Musslimani ZH. Theory of coupled optical \mathcal{PT} -symmetric structures. Opt Lett 2007;32:2632-2634.
- [18] Musslimani ZH, Makris KG, El-Ganainy R, Christodoulides DN. Optical solitons in \mathcal{PT} periodic potentials. Phys Rev Lett 2008;100:030402.
- [19] Berry MV. Optical lattices with \mathcal{PT} -symmetry are not transparent. J Phys A: Math Theor 2008;41:244007.
- [20] Klaiman S, Günther U, Moiseyev N. Visualization of branch points in \mathcal{PT} -symmetric waveguides. Phys Rev Lett 2008;101:080402.
- [21] Bendix O, Fleischmann R, Kottos T, Shapiro B. Exponentially fragile \mathcal{PT} symmetry in lattices with localized eigenmodes. Phys Rev Lett 2009;103:030402.
- [22] Longhi S. Bloch oscillations in complex crystals with \mathcal{PT} symmetry. Phys Rev Lett 2009;103:123601.
- [23] Zezyulin DA, Kartashov YV, Konotop VV. Stability of solitons in \mathcal{PT} -symmetric nonlinear potentials. Europhys Lett 2011;96:64003.
- [24] Driben R, Malomed BA. Stability of solitons in parity-time-symmetric couplers. Opt Lett 2011;36:4323-4325.
- [25] Alexeeva NV, Barashenkov IV, Sukhorukov AA, Kivshar YS. Optical solitons in \mathcal{PT} -symmetric nonlinear couplers with gain and loss. Phys Rev A 2012;85:063837.
- [26] Nixon S, Ge L, Yang J. Stability analysis for solitons in \mathcal{PT} -symmetric optical lattices. Phys Rev A 2012;85:023822.
- [27] D'Ambroise J, Kevrekidis PG, Malomed BA. Staggered parity-time-symmetric ladders with cubic nonlinearity. Phys Rev E 2015;91:033207.
- [28] Yan Z, Wen Z, Konotop VV. Solitons in a nonlinear Schrödinger equation with \mathcal{PT} -symmetric potentials and inhomogeneous nonlinearity: Stability and excitation of nonlinear modes. Phys Rev A 2015;92:023821.
- [29] Kominis Y, Bountis T, Flach S. Stability through asymmetry: Modulationally stable nonlinear supermodes of asymmetric non-Hermitian optical couplers. Phys Rev 2017;95:063832.
- [30] Makris KG, El-Ganainy R, Christodoulides DN, Musslimani ZH. \mathcal{PT} symmetric periodic optical potentials. Int J Theor Phys 2011;50:1019-1041.
- [31] Guo A, Salamo GJ, Duchesne D, Morandotti R, Volatier-Ravat M, Aimez V, Siviloglou GA, Christodoulides DN. Observation of \mathcal{PT} -symmetry breaking in complex optical potentials. Phys Rev Lett 2009;103:093902.
- [32] Rüter CE, Makris KG, El-Ganainy R, Christodoulides DN, Segev M, Kip D. Observation of parity-time symmetry in optics. Nat Phys 2010;6:192-195.
- [33] Regensburger A, Bersch C, Miri MA, Onishchukov G, Christodoulides DN, Peschel U. Parity-time synthetic photonic lattices. Nature 2012;488:167-171.
- [34] Wimmer M, Regensburger A, Miri MA, Bersch C, Christodoulides DN, Peschel U. Observation of optical solitons in \mathcal{PT} -symmetric lattices. Nat Commun 2015;6:7782.

- [35] Chestnov IY, Demirchyan SS, Alodjants AP, Rubo YG, Kavokin AV. Permanent Rabi oscillations in coupled exciton-photon systems with \mathcal{PT} -symmetry. *Sci Rep* 2016;6:19551.
- [36] Schwarz L, Cartarius H, Musslimani ZH, Main J, Wunner G. Vortices in Bose-Einstein condensates with \mathcal{PT} -symmetric gain and loss. *Phys Rev* 2017;95:053613.
- [37] Alexeeva NV, Barashenkov IV, Rayanov K, Flach S. Actively coupled optical waveguides, *Phys. Rev. A* 2014;89:013848.
- [38] Kartashov YV, Konotop VV, Zezyulin DA. \mathcal{CPT} -symmetric spin-orbit-coupled condensate. *Europhys Lett* 2014;107:50002.
- [39] Dana B, Bahabad A, Malomed BA. \mathcal{CP} symmetry in optical systems. *Phys. Rev. A* 2015;91:043808.
- [40] Kirikchi OB, Malomed BA, Karjanto N, Kusdiantara R, Susanto H. Solitons in a chain of charge-parity-symmetric dimers. *Phys. Rev. A* 2018;98:063841.
- [41] Konotop VV, Yang J, Zezyulin DA. Nonlinear waves in \mathcal{PT} -symmetric systems. *Rev Mod Phys* 2016;88:035002.
- [42] Suchkov SV, Sukhorukov AA, Huang JH, Dmitriev SV, Lee C, Kivshar YS. Nonlinear switching and solitons in \mathcal{PT} -symmetric photonic systems. *Laser Photonics Rev* 2016;10:177-213.
- [43] Yang J. Necessity of \mathcal{PT} symmetry for soliton families in one-dimensional complex potentials. *Phys Lett A* 2014;378:367-373.
- [44] Vanin EV, Korytin AI, Sergeev AM, Anderson D, Lisak M, Vázquez L. Dissipative optical solitons. *Phys Rev A* 1994;49:2806-2811.
- [45] Wright EM, Stegeman GI, Wabnitz S. Solitary-wave decay and symmetry-breaking instabilities in two-mode fibers. *Phys. Rev. A* 1989;40:4455.
- [46] Paré C, Florjańczyk M. Approximate model of soliton dynamics in all-optical fibers. *Phys. Rev. A* 1990;41:6287-6295.
- [47] Maimistov AI. Propagation of a light pulse in nonlinear tunnel-coupled optical waveguides. *Sov J Quantum Electron* 1991;21:687-690.
- [48] Romagnoli M, Trillo S, Wabnitz S. Soliton switching in nonlinear couplers. *Opt Quantum Electron* 1992;24:1237-1267.
- [49] Malomed BA. Solitons and nonlinear dynamics in dual-core optical fibers. In: Peng G-D. *Handbook of Optical Fibers*, Springer; 2018.
- [50] Chu PL, Malomed BA, Peng GD, Skinner I. Soliton dynamics in periodically modulated directional couplers. *Phys. Rev. E* 1994;49:5763-5767.
- [51] Malomed BA. *Soliton Management in Periodic Systems*. New York: Springer; 2006.
- [52] Turitsyn SK, Bale BG, Fedoruk MP. Dispersion-managed solitons in fibre systems and lasers. *Phys. Rep.* 2012;521:135-203.
- [53] Fibich G. *The Nonlinear Schrödinger Equation: Singular Solutions and Optical Collapse*. Heidelberg: Springer; 2015.
- [54] Towers I, Malomed BA. Stable (2+1)-dimensional solitons in a layered medium with sign-alternating Kerr nonlinearity. *J. Opt Soc Am B* 2002;19:537-543.
- [55] Abdullaev FK, Caputo JG, Kraenkel RA, Malomed BA. Controlling collapse in Bose-Einstein condensation by temporal modulation of the scattering length. *Phys Rev A* 2003;67:013605.
- [56] Saito H, Ueda M. Dynamically Stabilized Bright Solitons in a Two-Dimensional Bose-Einstein Condensate. *Phys Rev Lett* 2003;90:040403.
- [57] Driben R, Malomed BA. Stabilization of solitons in \mathcal{PT} models with supersymmetry by periodic management. *Europhys Lett* 2011;96:51001.
- [58] Abdullaev FK, Galimzyanov RM. Optical solitons in periodically managed \mathcal{PT} -symmetric media. *Optik* 2018;157:353-359.
- [59] Alexeeva NV, Barashenkov IV, Kivshar YS. Solitons in \mathcal{PT} -symmetric ladders of optical waveguides. *New J Phys* 2017;19:113032.
- [60] Campbell DK, Peyrard M, Sodano P. Kink-antikink interactions in the double sine-Gordon equation. *Physica D* 1986;19:165.
- [61] Campbell DK, Schonfeld JF, Wingate CA. Resonance structure in kink-antikink interactions in φ^4 theory. *Physica D* 1983;9:1.
- [62] Kivshar YuS, Malomed BA. Dynamics of solitons in nearly integrable systems. *Rev Mod Phys* 1989;61:763-915.